Titanium dioxide nanoparticles exacerbate allergic airway inflammation via TXNIP upregulation in a mouse model of asthma

Je-Oh Lim
Chonnam National University
Se-Jin Lee
Chonnam National University
Woong-Il Kim
Chonnam National University
So-Won Pak
Chonnam National University
Changjong Moon
Chonnam National University
In-Sik Shin
Chonnam National University
Jeong-Doo Heo (jdher@kitox.re.kr)
Korea Institute of Toxicology
Jong-Choon Kim
Chonnam National University https://orcid.org/0000-0002-8265-9911

Research

Keywords: Titanium dioxide nanoparticle, Asthma, Airway inflammation, Thioredoxin-interacting protein, Apoptosis

Posted Date: August 3rd, 2021

DOI: https://doi.org/10.21203/rs.3.rs-754255/v1

Abstract

Background

Titanium dioxide nanoparticles (TiO_2NPs) are widely used in the fields of industry and medicine and in various consumer products. With the increasing use of TiO_2NPs, there has been an increase in the number of toxicity studies; however, studies investigating the mechanism underlying its toxicity are very rare. In this study, we evaluated the potential toxic effects of TiO_2NPs exposure on the lungs as well as the development of asthma in ovalbumin (OVA)-induced mouse model of asthma. We also investigated the related toxic mechanism.

Results

TiO_2NPs caused pulmonary toxicity by exacerbating the inflammatory response, indicated by an increase in the number of inflammatory cells and levels of inflammatory mediators. Exposure of mice with OVA-induced asthma to TiO_2NPs led to significant increases in inflammatory mediators, cytokines, and airway hyperresponsiveness compared with non-exposed mice with asthma. This was also accompanied by an increase in inflammatory cell infiltration and mucus production in the lung tissues. TiO_2NPs also decreased the expression of B-cell lymphoma 2 (Bcl2) and increased the expression of thioredoxin-interacting protein (TXNIP), phospho-apoptosis signal-regulating kinase 1, Bcl2-associated X, and cleaved-caspase 3 in the lungs of asthmatic mice compared with those of non-exposed asthmatic mice. These responses were consistent with *in vitro* results obtained using human airway epithelial cells. TiO_2NPs treated cells exhibited an increase in the mRNA and protein expression of IL-1β, IL-6, and TNF-α with an elevation of TXNIP signaling compared to non-treated cells. Moreover, pathophysiological changes induced by TiO_2NPs treatment were significantly decreased by TXNIP knockdown in the airway epithelial cells.

Conclusion

Taken together, TiO_2NPs exposure induced toxicological changes in the respiratory tract and exacerbated the development of asthma via activation of the TXNIP-apoptosis pathway. These results provide insights into the mechanism underlying TiO_2NPs-mediated respiratory toxicity.

Background

Air pollutants, such as yellow dust and fine dust, have become a critical social issue and are life-threatening to patients with respiratory diseases. In particular, titanium dioxide nanoparticles (TiO_2NPs), a component of Asian dust and air pollutants, have been reported to exacerbate respiratory distress in several studies [1–4]. Moreover, TiO_2NPs induce an intensive inflammatory response by triggering

inflammatory cell migration and pro-inflammatory cytokine secretion, and consequently, contributing to the development and exacerbation of respiratory diseases [5, 6]. However, the mechanisms of action associated with the toxic effects of titanium on the respiratory system and its diseases have not been clearly identified.

Of the known respiratory disease, asthma is an inflammatory disease of the respiratory airways that affects proximately 300 million people globally [7]. It is characterized by excessive inflammation of the bronchi and obstruction of the airflow due to increased immune responses, resulting in varying respiratory symptoms, mainly difficulty breathing, wheezing, coughing and tightness in the chest [3, 8, 9]. Proinflammatory cytokines are a key player in the development and progression of asthma, and they induce elevated immune responses, resulting in characteristic responses in asthma, such as eosinophilia, airway hyperresponsiveness and mucus production [10]. Previous studies have shown that fine dust and air pollutants contribute to asthma exacerbation; however, the mechanism underlying the toxicity is not well established.

Thioredoxin-interacting protein (TXNIP), a critical regulator of pathological responses, is induced by various of stressors, including inflammation, metabolic dysfunction, apoptosis, and lung dysfunction [11–13]. TXNIP is expressed in the lungs of experimental animals exposed to lipopolysaccharide and ovalbumin (OVA), which induce increased inflammatory responses via the activation of inflammasomes [14–16]. In contrast, TXNIP is involved in the apoptotic response of lung tissues. Elevation of TXNIP expression by various stimuli results in the activation of apoptotic signaling molecules, such as mitochondrial apoptosis signal-regulating kinase 1 (ASK1), B-cell lymphoma 2 associated X (Bax), p38 mitogen-activated protein kinase and cleaved-caspase 3 (Cas3), which eventually trigger the apoptosis of lung tissues [17, 18]. The association between TiO_2NPs and apoptosis under asthmatic conditions has not been well established. Therefore, an in-depth study is needed to understand the apoptosis mechanisms triggered via TXNIP in OVA-induced mice and how TiO_2NPs pathologically exacerbate the development of asthma.

In this study, we investigated the exacerbation of asthma in response to TiO_2NPs exposure in OVA-induced asthmatic mice and explored the underlying mechanisms involving TXNIP and apoptosis.

Results

Physicochemical characterization of TiO_2NPs

The morphology, primary size, and hydrodynamic size of TiO_2NPs are shown in Fig. 1. The primary size and hydrodynamic size in phosphate-buffered saline (PBS) were 48.89 ± 15.49 and 238.94 ± 57.94 nm, respectively. The specific surface area of TiO_2NPs was 40.45 and 39.38 m^2/g as determined using Brunauer–Emmett–Teller (BET) and single point methods, respectively (Table 1). The zeta potential of the TiO_2NPs was − 31.01 mV (Fig. 1c). Purity of TiO_2NPs was measured as 21.35% of Ti and 78.65% of O

using energy-dispersive X-ray spectroscopy (Fig. 1d). TiO_2NPs suspensions did not show detectable endotoxin levels (data not shown). TiO_2NPs concentrations in the lung tissues were determined using inductively coupled plasma mass spectrometry (ICP-MS) (Table 1); the amount of TiO_2NPs in TiO_2NPs-treated groups was markedly increased in a dose-dependent manner compared with that in the vehicle control (VC) group.

Table 1
Measurement of surface area and ICP-MS of TiO_2NPs.

BET Surface area (m^2/g)	**ICP-MS (mg/g)**				
40.45	**VC**		**TiO_2NPs 5**	**TiO_2NPs 10**	**TiO_2NPs 20**
	0.38 ± 0.032		2.88 ± 0.311	5.68 ± 0.597	6.69 ± 0.613
Single point Surface area (m^2/g)	**VC**	**OVA**	**OVA+ TiO_2NPs 5**	**OVA+ TiO_2NPs 10**	**OVA+ TiO_2NPs 20**
39.38	0.34 ± 0.056	0.32 ± 0.042	2.53 ± 0.397	6.43 ± 0.617	7.94 ± 0.673

Effects of TiO_2 NPs on hyperresponsiveness (AHR) and inflammatory cell counts

In pulmonary toxicity study, exposure to TiO_2NPs significantly increased inflammatory cell counts in the bronchoalveolar lavage fluid (BALF) of mice compared with the BALF of VC mice. In particular, a marked increase in the number of neutrophils and macrophages was observed (Fig. S1). BALF of the OVA group showed increased inflammatory cell counts, especially that of eosinophils, which was significantly increased compared with the VC group (Fig. 2a). OVA-induced mice exposed to TiO_2NPs exhibited elevated counts of eosinophils, macrophages, and neutrophils compared with the OVA group, and this increase occurred in a dose-dependent manner. As shown in Fig. 2b, the mean Penh value was augmented in the OVA group compared with the VC group. In addition, Penh values increased in OVA + TiO_2NPs mice compared with OVA mice, and this increase was dose-dependent (Fig. 2b).

Effects of TiO_2 NPs on cytokine production and OVA-specific IgE levels in serum

To determine whether TiO_2NPs affect the production of inflammatory cytokines in addition to increasing the number of inflammatory cells, the cytokine levels in BALF samples were measured. In pulmonary toxicity study, the levels of proinflammatory cytokines, namely tumor necrosis factor (TNF)-α, interleukin (IL)-6, and IL-1β, were significantly increased in TiO_2NPs-treated groups compared with the VC group (Fig. S2). The levels of TNF-α, IL-6, and IL-1β in BALF were significantly increased in OVA group compared with the VC group. Exposure to TiO_2NPs increased the levels of TNF-α, IL-6, and IL-1β compared with the OVA group, and this increase was dose-dependent (Fig. 3a-c). Similar to the levels of TNF-α, IL-6, and IL-1β, the levels of IL-5 and IL-13 in BALF were increased in the OVA group. Moreover, the levels of IL-5 and IL-13

were increased dose-dependently in TiO_2NPs-treated groups compared with the OVA group (Fig. 3d and e). The OVA-specific IgE level in serum was elevated in the TiO_2NPs-treated groups compared with the OVA group (Fig. 3f).

Effects of TiO_2 NPs on airway inflammation and mucous secretion in OVA-induced mice

Mice exposed to TiO_2NPs showed an accumulation of inflammatory cells around the alveoli and bronchi as well as increased mucus production (Fig. S3). OVA-induced mice showed a significantly higher degree of airway inflammation then VC mice. When the OVA-induced mice were treated with TiO_2NPs, airway inflammation worsened in a dose-dependent manner compared to that in OVA mice (Fig. 4a). Changes in the mucus production index exhibited a pattern similar to changes in airway inflammation wherein mucus production in TiO_2NPs-treated groups was markedly increased in a dose-dependent manner compared with that in the OVA group (Fig. 4b).

Effects Of Tionps On Txnip And Apoptotic Protein Expression

Immunohistochemistry (IHC) was used to estimate the expression levels of TXNIP and cleaved- Cas3 in lung tissues in response to OVA and TiO_2NPs treatment. The lungs of normal mice exposed to TiO_2NPs showed a dose-dependent increase in the expression of TXNIP and cleaved-Cas3 compared with those of VC mice. Similarly, exposure to TiO_2NPs led to increases in the expression of TXNIP, phospho-ASK1 (p-ASK1), Bax, and cleaved-Cas3 and a decrease in the expression of B-cell lymphoma 2 (Bcl2) compared with that in VC mice (Fig. S4). TXNIP expression in the OVA group was increased compared with that in the VC group. TXNIP expression increased in a dose-dependent manner in TiO_2NPs-treated groups compared with the OVA group (Fig. 5a). Likewise, cleaved-Cas3 expression in the OVA group increased compared with that in the VC group and in the TiO_2NPs-treated groups compared with that in the OVA group (Fig. 5b). The effects of TiO_2NPs on TXNIP activation were determined using immunoblotting. As shown in Fig. 6a and b, TXNIP expression in the lungs was increased in the OVA group compared with the VC group. The expression of p-ASK1, Bax, and cleaved-Cas3 in the OVA group was also increased compared with that in the VC group. However, Bcl2 expression decreased in OVA group compared with the VC group. Compared with the OVA group, exposure to TiO_2NPs induced a marked increase in the expression of TXNIP, p-ASK1, Bax, and cleaved-Cas3 in a dose-dependent manner. The Bcl2 level in TiO_2NPs-treated groups was lower than that in the OVA group.

Effects of TiO_2 NPs on the production of proinflammatory mediators in NCI-H292 cells

For the *in vitro* experiments, concentrations of TiO_2NPs for treatment groups were decided based on the results of the cell viability assay (Fig. 7a). TiO_2NPs treatment significantly elevated the levels of IL-1β, IL-6, and TNF-α in NCI-H292 cells in a dose-dependent manner compared to untreated cells (Fig. 7b-d).

As shown in Fig. 8a-d, real-time reverse-transcription polymerase chain reaction (qRT-PCR) results revealed that the expression of *IL-1β*, *IL-6*, *IL-8*, and *TNF-α* was markedly increased in a dose-dependent

manner in NCI-H292 cells treated with TiO_2NPs compared with those in the control group.

Effects of TiO_2 NPs on TXNIP and apoptosis protein expression in NCI-H292 cells

Immunoblotting revealed that TXNIP expression increased in TiO_2NPs-treated cells compared to untreated cells, and this increase occurred in a dose-dependent manner. TiO_2NPs treatment also led to an increase in the levels of p-ASK1, Bax, and cleaved-Cas3 compared to untreated cell, this also occurred in a dose-dependent manner (Fig. 9a and b). To determine the role of TXNIP in mediating the effects of TiO_2NPs, we transfected NCI-H292 cells with *TXNIP*-specific small interfering RNA (siRNA). The control siRNA did not have any effect on the increased expression of p-ASK1, Bax and cleaved-Cas3 and decreased Bcl2 expression seen with TiO_2NPs treatment; however, treatment with *TXNIP*-specific siRNA decreased the expression of Bax and cleaved-Cas3 and increased the expression of Bcl2 in TiO_2NPs-treated cells, restoring them to levels similar to those of the control group (Fig. 10a and b).

Discussion

There has been an increase in the number of patients with underlying respiratory diseases, and they are a vulnerable subpopulation that should be considered when evaluating the potential respiratory toxicity of various substances [19]. The aim of this study was to examine the effect of TiO_2NPs on asthma exacerbation and elucidate the mechanism that underlies this aggravation. We showed that exposure to TiO_2NPs aggravated asthma, increased TXNIP expression, and activated apoptosis in the lungs of OVA-induced mice. In addition, TiO_2NPs treatment of NCI-H292 cells led to an upregulation of apoptotic machinery via upregulation in TXNIP.

In this study, exposure to TiO_2NPs was found to increase the inflammatory response in the respiratory tract and worsen the major symptoms of asthma, namely, airway inflammation, mucus overproduction, and AHR, in mice with OVA-induced asthma. Eosinophilic inflammatory response, which is characteristic of asthma, is known to be induced by IL-4, IL-5, and IL-13 produced by $CD4^+$ T helper type 2 (Th2) cells [20]. In addition, proinflammatory cytokines, such as TNF-α, IL-6, and IL-1β, function as growth factors for B cells and play an important role in the differentiation of $CD4^+$ Th2 cells [21]. These cytokines have been reported to increase the secretion of mucus by stimulating the goblet cells of bronchi, resulting in AHR [22, 23]. Asthmatic mice exposed to TiO_2NPs showed a characteristic increase in cytokines, and the aforementioned major symptoms of asthma further worsened. In NCI-H292 cells treated with TiO_2NPs, cytokine production was significantly increased, similar to our *in vivo* results. Thus, we demonstrated that TiO_2NPs cause respiratory toxicity and exacerbate asthma; this is in conformity with previous reports [1, 6, 24].

TXNIP can directly bind to thioredoxin (TRX) and inhibit TRX function, leading to the activation of apoptotic signaling pathway. Under normal conditions, TRX inhibits the activation of ASK1 via formation of a complex with ASK1. However, activated TXNIP induces the dissociation of this TRX-ASK1 complex,

resulting in the activation of ASK1 and, consequently, apoptosis [25, 26]. The association between nanoparticles and TXNIP has been reported in several studies [14, 15]. For example, exposure to silica dioxide nanoparticles has been shown to exacerbate asthma and increase pulmonary toxicity via upregulation of TXNIP. In this study, exposure to TiO_2NPs increased TXNIP expression and activated TXNIP downstream signaling in the lungs of normal and asthmatic mice. Furthermore, we found that the TiO_2NPs-activated apoptosis was suppressed by down-regulation of the TXNIP gene in human airway epithelial cells. In contrast, upregulation of TXNIP promotes apoptosis by increasing the Bax/Bcl2 ratio and cleaved-caspase 3 expression [18]. Taken together, exposure of mice to TiO_2NPs increases the expression of TXNIP in the lungs, demonstrating that TXNIP may be involved in the molecular pathogenesis of asthma. This suggests that TXNIP may be responsible for the aggravating effect of TiO_2NPs-induced apoptosis in asthmatic lungs.

Conclusion

In light of the corona virus disease of 2019 pandemic, interest in respiratory-related diseases is increasing, and the prevention and management of underlying respiratory diseases has become more important. In this study, we showed that TiO_2NPs induced respiratory toxicity and exacerbated asthma via TXNIP upregulation. Underlying diseases of the respiratory system can be further exacerbated by various environmental allergens such as viruses, house dust mites, and air pollutants. Thus, not only patients, but also normal people may suffer health disorders. As mentioned above, TiO_2NPs may contribute to the development of respiratory diseases and is life-threatening as it reduces resistance to environmental allergens by exacerbating any underlying respiratory disease. Therefore, this study presents toxicological information about TiO_2NPs, which has not been previously reported, and provides evidence for the toxicological mechanism underlying TiO_2NPs-mediated respiratory toxicity and diseases.

Methods

Characterization of TiO_2NPs

TiO_2NPs were purchased from Sigma-Aldrich (particle size < 25 nm, 637254, St. Louis, MO, USA). We quantified the morphology and size of TiO_2NPs using transmission electron microscopy (JEM-1210, JEOL, Tokyo, Japan) at an accelerating voltage of 200 kV and scanning electron microscopy (Zeiss EVO-MA10; Carl Zeiss Meditec AG, Jena, Germany) at an accelerating voltage of 15 kV. The specific surface area of TiO_2NPs was measured by nitrogen absorption methods based on the multipoint BET method (ASAP2020; Micromeritics, Norcross, GA, USA). The hydrodynamic size and zeta potential of TiO_2NPs were determined by ELS-8000 (Otsuka Electronic, Tokyo, Japan). The purity of TiO_2NPs used in the experiment were determined by energy-dispensive X-ray spectoroscopy (Rayny EDX-700, Shimadzu). The endotoxin levels in TiO_2NPs suspension were determined using a Pierce LAL Chromogenic Endotoxin Quantitation Kit (Thermo Fisher Scientific, Waltham, MA, USA). After completion of treatment procedures,

lung tissue was harvested, weighed, and digested overnight with concentrated nitric acid, and the resultant samples were analyzed for elemental TiO_2NPs using ICP-MS (Perkin Elmer, Waltham, MA, USA).

Experimental procedure for allergic asthma induction

Specific pathogen-free female BALB/c mice (6 weeks old) were purchased from Samtako Co. (Osan, Republic of Korea) quarantined and acclimatized for seven days. The animals were maintained at 22 ± 2 °C in a room with a relative humidity of 50 ± 5%, artificial lighting from 08:00–20:00, and 13–18 air changes per hour. Animals were provided with *ad libitum* access to a standard laboratory diet and water. All experimental procedures were carried out in accordance with the National Institute Health Guidelines for the Care and Use of Laboratory Animals. The Institutional Animal Care and Use Committee of Chonnam National University approved experimental protocols involving animals (CNU IACUC-YB-2020-19).

To investigate pulmonary toxicity of TiO_2NPs, twenty-four healthy female mice were randomly assigned to four experimental groups (n = 6 per group); VC group and three TiO_2NPs-treated (5, 10, and 20 mg/kg, respectively) groups. On day 1, 3, and 5, animals of the TiO_2NPs treated groups (5, 10, and 20 mg/kg doses in 50 μL of PBS, respectively) received TiO_2NPs via intranasal instillation under light anesthesia using Zoletil 50® (Virbac Laboratories, Carros, France). The VC group received 50 μL of PBS via intranasal instillation. TiO_2NPs were prepared in PBS and sonicated in an ultrasonicator (VCX-130, Sonics and Materials, Newtown, CT) for 3 min (130 W, 20 kHz, pulse 59/1) before intranasal instillation.

To investigate the effect of TiO_2NPs on the development of asthma, 30 animals were randomly assigned to five experimental groups (each group, n = 6); VC group, OVA group, and three OVA+ TiO_2NPs (5, 10, and 20 mg/kg) groups. On day 1 and 15, mice were sensitized with an intraperitoneal injection of 20 μg of OVA (Sigma-Aldrich) emulsified with 2 mg of aluminum hydroxide (Thermo Scientific) in 200 μL of PBS (pH 7.4). On day 22, 24, and 26, the mice received a 1 h airway challenge with 1% (w/v) OVA solution aerosolized using an ultrasonic nebulizer (NE-U12; Omron Corp., Tokyo, Japan). On day 21, 23, and 25, animals of the TiO_2NPs treatment groups (5, 10, and 20 mg/kg doses in 50 μL of PBS, respectively) received TiO_2NPs via intranasal instillation under light anesthesia using Zoletil 50® (Virbac Laboratories). The VC and OVA groups received 50 μL of PBS via intranasal instillation. TiO_2NPs were prepared in PBS and sonicated in an ultrasonicator for 3 min before intranasal instillation.

Measurement of airway AHR

Penh values were indirectly assessed at 24 h after the final intranasal instillation via single-chamber whole body plethysmography (Allmedicus, Seoul, Republic of Korea). Briefly, mice were anesthetized with an intraperitoneal injection of a mixture of Zoletil and Xylazine (40 mg/kg and 10 mg/kg, respectively), placed in a chamber, and nebulized with aerosolized PBS or methacholine in increasing concentrations (10, 20, and 40 mg/mL).

Collection of BALF and cell counting

Mice were sacrificed at 24 h after measurement of AHR via an intraperitoneal injection of Zoletil 50® (Virbac Laboratories), and a tracheostomy was performed. To obtain BALF, ice-cold PBS (0.7 mL) was infused into the lungs twice and was withdrawn each time using a tracheal cannula (a total volume of 1.4 mL). The BALF samples were centrifuged, and its supernatant was collected for biochemical analysis. Collected cells were resuspended in ice-cold PBS (0.5 mL), and 200 μL of the resuspended solution was centrifuged (200 g, 4 °C, 10 min) onto slides using a Cytospin (Hanil Science Industrial Co., Ltd., Seoul, Republic of Korea). The slides were dried, and the cells were fixed and stained. Differential cell counts were performed using the Diff-Quik® staining reagent (Sysmex Corporation, Kobe, Japan) according to the manufacturer's instructions.

Cytokines assay

The levels of several cytokines, namely TNF-α, IL-6, IL-1β, IL-5, and IL-13, were measured in BALF using commercial enzyme-linked immunosorbent assay (ELISA) kits (BD Biosciences, San Jose, CA, USA) according to the manufacturer's protocol. The serum level of OVA-specific IgE was measured using an ELISA kit (BioLegend, San Diego, CA, USA). Absorbance was measured at 450 nm using an ELISA reader (Bio-Rad Laboratories, Hercules, CA, USA).

Histopathology and IHC

After BALF samples were collected, the lung tissue was fixed with 4% (v/v) paraformaldehyde for 48 h. The tissues were paraffin-embedded, sectioned at a thickness of 4 μm and stained using hematoxylin and eosin (Sigma-Aldrich) or periodic acid-Schiff solution (IMEB Inc., San Marcos, CA, USA) to evaluate airway inflammation and mucus production, respectively. In addition, the sectioned tissues were processed for IHC, as previously described (Lim et al., 2020b). Primary antibodies used for detection of protein expression were anti-TXNIP (NBP1-54578; 1:200 dilution; Novus Biologicals, Littleton, CO, USA) and anti-cleaved-Cas3 (#9661; 1:200 dilution; Cell signaling, Danvers, MA, USA). Each slide was examined manually by investigators blind to the treatment groups using a light microscope (Leica, Wetzlar, Germany) with 10 and 20x objective lenses and a 100x oil immersion lens. Ten randomly selected nonoverlapping areas per slide were captured with a digital camera (IMTcamCCD5; IMT Inc., Daejeon, Republic of Korea), and quantitative analyses of airway inflammation, mucus production, and protein expression were performed using an image analyzer (IMT i-Solution software, Vancouver, BC, Canada).

Western blot analysis

To quantify protein expression, we performed immunoblotting as previously described [27]. Primary antibodies used are as follows: anti-TXNIP (NBP1-54578; Novus Biologicals), anti-p-ASK1 (SAB4504337; Sigma-Aldrich), anti-total-ASK1 (t-ASK1, ab45178; Abcam, Cambridge, UK), anti-Bcl2 (#2876; Cell signaling), anti-Bax (#2772; Cell signaling), anti-cleaved-Cas3 (#9661; Cell signaling), and anti-β-actin (β-

act, #4967; Cell signaling). Densitometric analysis of expression was performed using Chemi-Doc (Bio-Rad Laboratories).

Cell culture

The human airway epithelial cell line NCI-H292 was obtained from the American Type Culture Collection (Manassas, VA, USA). The cells were grown in RPMI 1640 medium (WELGENE, South Korea) with 10% fetal bovine serum, streptomycin (100 µg/mL), and penicillin (100 U/mL) and incubated in a humidified chamber maintained at 37 °C with 5% CO_2. The cells were serum-starved for 1 h before use.

Cell viability assay

Cell viability was performed using an EZ-Cytox cell viability assay kit (DAELIL lab, Seoul, Republic of Korea). Briefly, NCI-H292 cells were seeded in 96 well-plate (4×10^4 cells/well). After 24 h, the medium was replaced with fresh medium, and various concentrations of TiO_2NPs (1.56, 3.13, 6.25, 12.5, 25 µg/mL) were added. The culture plate was incubated for another 24 h. Subsequently, the viable cells were determined by adding 10 µL of the kit solution to each well and incubating for 4 h. Absorbance was measured at 450 nm using an ELISA reader (Bio-Rad Laboratories).

Measurement of mRNA expression of proinflammatory cytokines in NCI–H292 cells

To quantify proinflammatory cytokines mRNA expression, we measured using qRT-PCR as described previously [28]. qRT-PCR experiments were performed using specific forward and reverse primers (Table S1).

Small interfering RNA transfection of NCI-H292 cells

TXNIP-specific siRNA (4392420) and scrambled siRNA (4390843) were purchased from Ambion (Waltham, MA, USA). Each siRNA (20 nM) was transfected into NCI-H292 cells using LipofectamineTM RNAiMAX reagent (Invitrogen, Waltham, MA, USA) following the forward transfection method, as prescribed by the manufacturer. After suppression of endogenous TXNIP expression, the cells were treated with 25 µg/mL TiO_2NPs or PBS and harvested after 6 h. To investigate the protein expression involved in TXNIP-apoptosis signaling, western blot was performed as mentioned above.

Statistical analysis

Data are expressed as means ± standard deviation (SD). Statistical significance was determined using analysis of variance followed by Dunnett's test for multiple comparisons. *P* values less than 0.05 were considered statistically significant.

Abbreviations

TiO_2NPs: Titanium dioxide nanoparticles; TXNIP: Thioredoxin-interacting protein; OVA: Ovalbumin; ASK1: Apoptosis signal-regulating kinase 1; Bax: B-cell lymphoma 2 associated X; Cas3: Caspase 3; PBS: Phosphate-buffered saline; BET: Brunauer–Emmett–Teller; ICP-MS: Inductively coupled plasma mass spectrometry; VC: Vehicle control; AHR: Hyperresponsiveness; BALF: Bronchoalveolar lavage fluid; TNF-α: Tumor necrosis factor-α; IL: Interleukin; IHC: Immunohistochemistry; p-ASK1: Phospho-ASK1; t-ASK1: Total-ASK1; Bcl2: B-cell lymphoma 2; qRT-PCR: Real-time reverse-transcription polymerase chain reaction; siRNA: Small interfering RNA; Th2: T helper type 2; TRX: Thioredoxin; ELISA: Enzyme-linked immunosorbent assay; β-act: β-actin; SD: standard deviation.

Declarations

Acknowledgments

Not applicable.

Authors' contributions

J.O.L, S.J.L., W.I.K., S.W.P., and C.M. designed and performed the experiments, analyzed the data, and interpreted the results of experiments. J.D.H. and J.C.K. conceived and supervised the study. The manuscript was written by J.O.L. and I.S.S., and revised critically by J.C.K. All authors read and approved the final manuscript.

Funding

This work was supported by the National Research Foundation of Korea (NRF) grant funded by the Korea Government (MSIT) (NRF-2020R1A4A1019395).

Availability of data and materials

The data sets supporting the conclusions of this article are included within the article and its Additional files 1.

Ethics approval and consent to participate

All experimental procedures were carried out in accordance with the National Institute Health Guidelines for the Care and Use of Laboratory Animals. The Institutional Animal Care and Use Committee of Chonnam National University approved experimental protocols involving animals (CNU IACUC-YB-2020-19).

Consent for publication

Not applicable.

Competing interests

The authors declare that they have no competing interests.

Author details

[1] College of Veterinary Medicine and BK21 FOUR Program, Chonnam National University, 77 Yongbong-ro, Buk-gu, Gwangju 61186, Republic of Korea

[2] Bioenvironmental Science & Technology Division, Korea Institute of Toxicology, Jinju 52834, Republic of Korea

References

1. Jonasson S, Gustafsson A, Koch B, Bucht A. Inhalation exposure of nano-scaled titanium dioxide (TiO2) particles alters the inflammatory responses in asthmatic mice. Inhal Toxicol. 2013;25(4):179–91. https://doi.org/10.3109/08958378.2013.770939.
2. da Silva AL, Cruz FF, Rocco PRM, Morales MM. New perspectives in nanotherapeutics for chronic respiratory diseases. Biophys Rev. 2017;9(5):793–803. https://doi.org/10.1007/s12551-017-0319-x.
3. Ihrie MD, Bonner JC. The toxicology of engineered nanomaterials in asthma. Curr Environ Health Rep. 2018;5(1):100–9. https://doi.org/doi: 10.1007/s40572-018-0181-4.
4. Dasari KB, Cho H, Jaćimović R, Sun GM, Yim YH. Chemical composition of asian dust in daejeon, korea, during the spring season. ACS Earth Space Chem. 2020;4:1227–36. https://doi.org/10.1021/acsearthspacechem.9b00327.
5. Ambalavanan N, Stanishevsky A, Bulger A, Halloran B, Steele C, Vohra Y, et al. Titanium oxide nanoparticle instillation induces inflammation and inhibits lung development in mice. Am J Physiol Lung Cell Mol Physiol. 2013;304(3):L152–61. https://doi.org/10.1152/ajplung.00013.2012.
6. Kim BG, Lee PH, Lee SH, Park MK, Jang AS. Effect of TiO2 nanoparticles on inflammasome-mediated airway inflammation and responsiveness. Allergy Asthma Immunol Res. 2017;9(3):257–64. https://doi.org/10.4168/aair.2017.9.3.257.
7. Frey SM, Jones MR, Goldstein N, Riekert K, Fagnano M, Halterman JS. Knowledge of inhaled therapy and responsibility for asthma management among young teens with uncontrolled persistent asthma. Acad Pediatr. 2018;18(3):317–23. https://doi.org/10.1016/j.acap.2018.01.006.
8. Alharris E, Alghetaa H, Seth R, Chatterjee S, Singh NP, Nagarkatti M, et al. Resveratrol attenuates allergic asthma and associated inflammation in the lungs through regulation of miRNA-34a that targets FoxP3 in mice. Front Immunol. 2018;9:2992. https://doi.org/10.3389/fimmu.2018.02992.
9. Menzel M, Ramu S, Calvén J, Olejnicka B, Sverrild A, Porsbjerg C, et al. Oxidative stress attenuates TLR3 responsiveness and impairs anti-viral mechanisms in bronchial epithelial cells from COPD and asthma patients. Front Immunol. 2019;10:2765. https://doi.org/10.3389/fimmu.2019.02765.
10. Kim HY, DeKruyff RH, Umetsu DT. The many paths to asthma: phenotype shaped by innate and adaptive immunity. Nat Immunol. 2010;11(7):577–84. https://doi.org/10.1038/ni.1892.

11. Lerner AG, Upton JP, Praveen PV, Ghosh R, Nakagawa Y, Igbaria A, et al. IRE1alpha induces thioredoxin-interacting protein to activate the NLRP3 inflammasome and promote programmed cell death under irremediable ER stress. Cell Metab. 2012;16(2):250–64. https://doi.org/10.1016/j.cmet.2012.07.007.
12. Abdelsaid MA, Matragoon S, Ergul A, El-Remessy AB. Deletion of thioredoxin interacting protein (TXNIP) augments hyperoxia-induced vaso-obliteration in a mouse model of oxygen induced-retinopathy. PLoS One. 2014;9(10):e110388. https://doi.org/10.1371/journal.pone.0110388.
13. Mohamed IN, Sarhan NR, Eladl MA, El-Remessy AB, El-Sherbiny M. Deletion of thioredoxin-interacting protein ameliorates high fat diet-induced non-alcoholic steatohepatitis through modulation of toll-like receptor 2-NLRP3-inflammasome axis: Histological and immunohistochemical study. Acta Histochem. 2018;120(3):242–54. https://doi.org/10.1016/j.acthis.2018.02.006.
14. Ko JW, Shin NR, Lim JO, Jung TY, Moon C, Kim TW, et al. Silica dioxide nanoparticles aggravate airway inflammation in an asthmatic mouse model via NLRP3 inflammasome activation. Regul Toxicol Pharmacol. 2020;112:104618. https://doi.org/10.1016/j.yrtph.2020.104618.
15. Lim JO, Ko JW, Jung TY, Kim WI, Pak SW, Shin IS, et al. Pulmonary inflammation caused by silica dioxide nanoparticles in mice via TXNIP/NLRP3 signaling pathway. Mol Cell Toxicol. 2020;16:245–52. https://doi.org/10.1186/s13273-020-00080-y.
16. Zhou W, Shao W, Zhang Y, Liu D, Liu M, Jin T. Glucagon-like peptide-1 receptor mediates the beneficial effect of liraglutide in an acute lung injury mouse model involving the thioredoxin-interacting protein. Am J Physiol Endocrinol Metab. 2020;319(3):E568–78. https://doi.org/10.1152/ajpendo.00292.2020.
17. Chihara Y, Iizumi Y, Horinaka M, Watanabe M, Goi W, Morita M, et al. Histone deacetylase inhibitor OBP–801 and amrubicin synergistically inhibit the growth of squamous cell lung carcinoma by inducing mitochondrial ASK1–dependent apoptosis. Int J Oncol. 2020;56(3):848–56. https://doi.org/10.3892/ijo.2020.4969.
18. Deng W, Li Y, Jia Y, Tang L, He Q, Liu D. Over-expression of thioredoxin-interacting protein promotes apoptosis of MIN6 cells via activating p38MAPK pathway. Xi Bao Yu Fen Zi Mian Yi Xue Za Zhi. 2017;33(10):1323–7.
19. Izquierdo JL, Almonacid C, González Y, Del Rio-Bermudez C, Ancochea J, Cárdenas R, et al. The impact of COVID-19 on patients with asthma. Eur Respir J. 2021;57(3):2003142. https://doi.org/10.1183/13993003.03142-2020.
20. Abdulnasser Harfoush S, Hannig M, Le DD, Heck S, Leitner M, Omlor AJ, et al. High-dose intranasal application of titanium dioxide nanoparticles induces the systemic uptakes and allergic airway inflammation in asthmatic mice. Respir Res. 2020;21(1):168. https://doi.org/10.1186/s12931-020-01386-0.
21. Ma J, Chan CC, Huang WC, Kuo ML. Berberine inhibits pro-inflammatory cytokine-induced IL-6 and CCL11 production via modulation of STAT6 pathway in human bronchial epithelial cells. Int J Med Sci. 2020;17(10):1464–73. https://doi.org/10.7150/ijms.45400.

22. Shi H, Magaye R, Castranova V, Zhao J. Titanium dioxide nanoparticles: a review of current toxicological data. Part Fibre Toxicol. 2013;10:15. https://doi.org/10.1186/1743-8977-10-15.
23. Tanabe T, Rubin BK. Airway goblet cells secrete pro-inflammatory cytokines, chemokines, and growth factors. Chest. 2016;149(3):714–20. https://doi.org/10.1378/chest.15-0947.
24. Mishra V, Baranwal V, Mishra RK, Sharma S, Paul B, Pandey AC. Titanium dioxide nanoparticles augment allergic airway inflammation and Socs3 expression via NF-kappaB pathway in murine model of asthma. Biomaterials. 2016;92:90–102. https://doi.org/10.1016/j.biomaterials.2016.03.016.
25. Hsieh CC, Papaconstantinou J. Thioredoxin-ASK1 complex levels regulate ROS-mediated p38 MAPK pathway activity in livers of aged and long-lived Snell dwarf mice. FASEB J. 2006;20(2):259–68. https://doi.org/10.1096/fj.05-4376com.
26. Malone CF, Emerson C, Ingraham R, Barbosa W, Guerra S, Yoon H, et al. mTOR and HDAC inhibitors converge on the TXNIP/thioredoxin pathway to cause catastrophic oxidative stress and regression of RAS-driven tumors. Cancer Discov. 2017;7(12):50–1463. https://doi.org/10.1158/2159-8290.CD-17-0177.
27. Shin IS, Shin NR, Park JW, Jeon CM, Hong JM, Kwon OK, et al. Melatonin attenuates neutrophil inflammation and mucus secretion in cigarette smoke-induced chronic obstructive pulmonary diseases via the suppression of Erk-Sp1 signaling. J Pineal Res. 2015;58(1):50–60. https://doi.org/10.1111/jpi.12192.
28. Lim JO, Shin NR, Seo YS, Nam HH, Ko JW, Jung TY, et al. Silibinin attenuates silica dioxide nanoparticles-induced inflammation by suppressing TXNIP/MAPKs/AP-1 signaling. Cells. 2020;9(3):678. https://doi.org/10.3390/cells9030678.

Figures

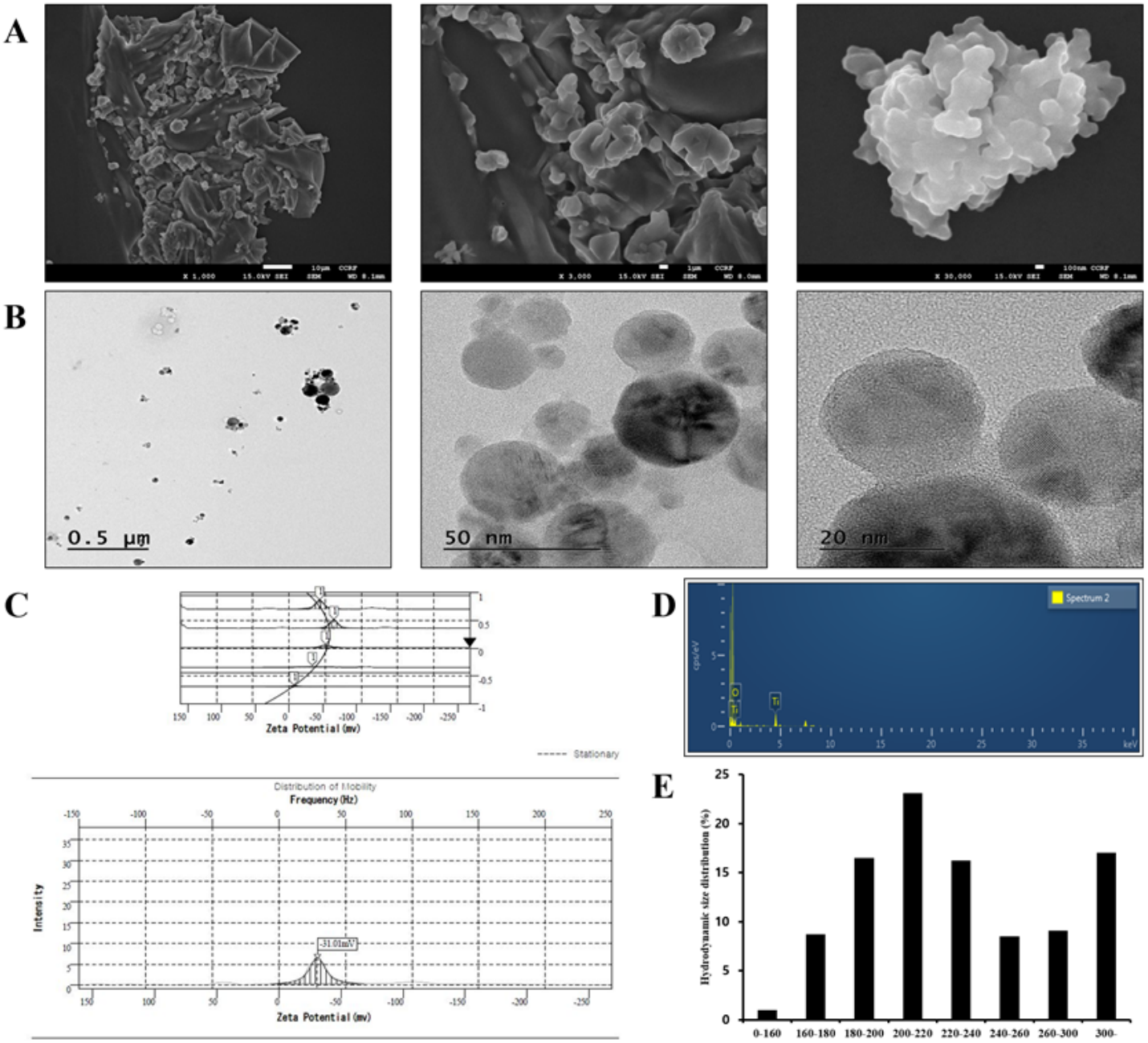

Figure 1

Morphology and physicochemical properties of TiO2NPs. a Morphology of TiO2NPs measured using transmission electron microscopy. b Morphology of TiO2NPs measured using scanning electron microscopy. c Zeta potential of TiO2NPs measured using ELS-8000 (-31 mV). d Purity of TiO2NPs measured using energy-dispersive X-ray spectroscopy (Ti: 21.35%, O: 78.65%). e Hydrodynamic size of TiO2NPs in PBS solution measured using ELS-8000.

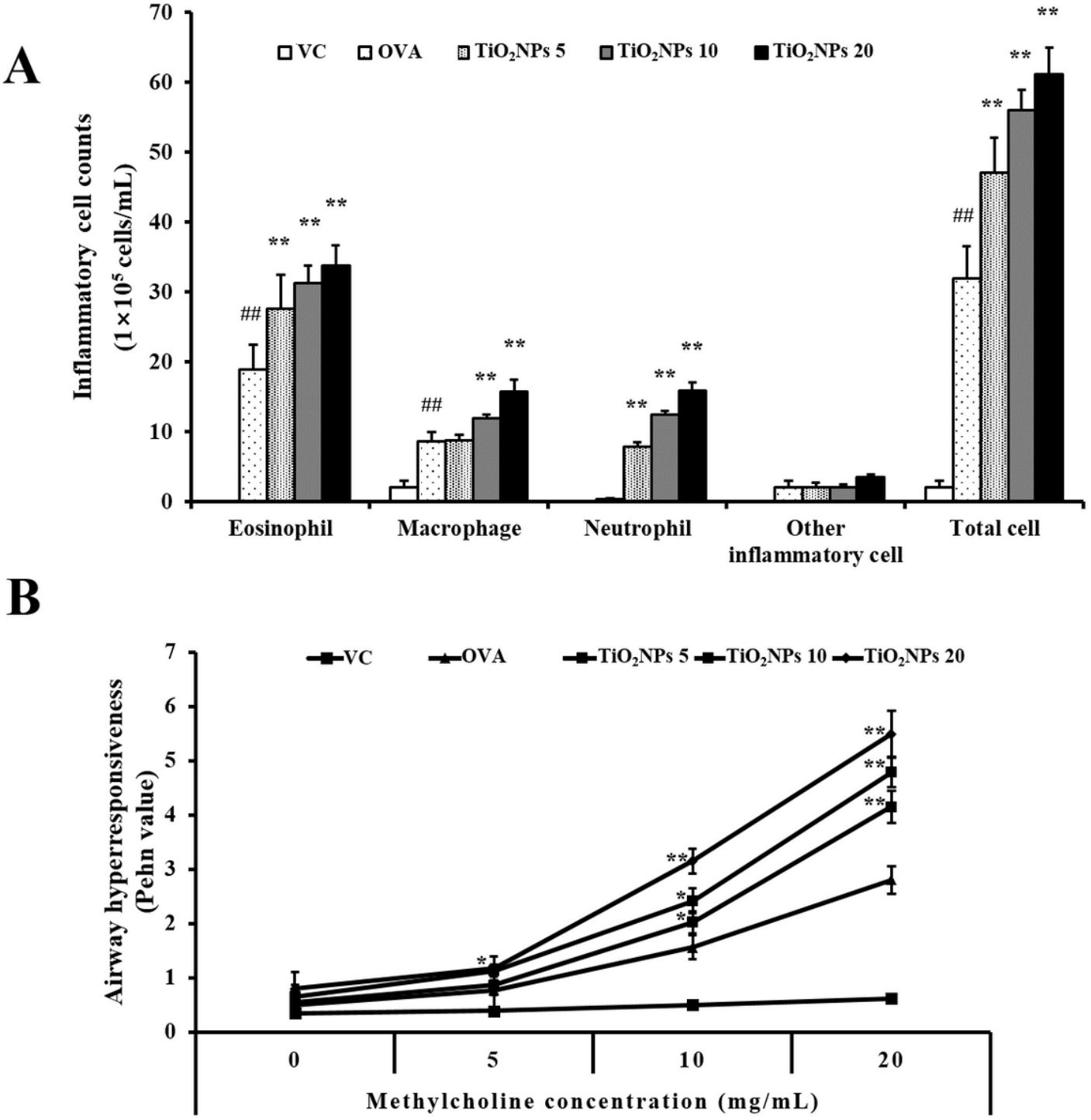

Figure 2

Morphology and physicochemical properties of TiO2NPs. a Morphology of TiO2NPs measured using transmission electron microscopy. b Morphology of TiO2NPs measured using scanning electron microscopy. c Zeta potential of TiO2NPs measured using ELS-8000 (-31 mV). d Purity of TiO2NPs measured using energy-dispersive X-ray spectroscopy (Ti: 21.35%, O: 78.65%). e Hydrodynamic size of TiO2NPs in PBS solution measured using ELS-8000.

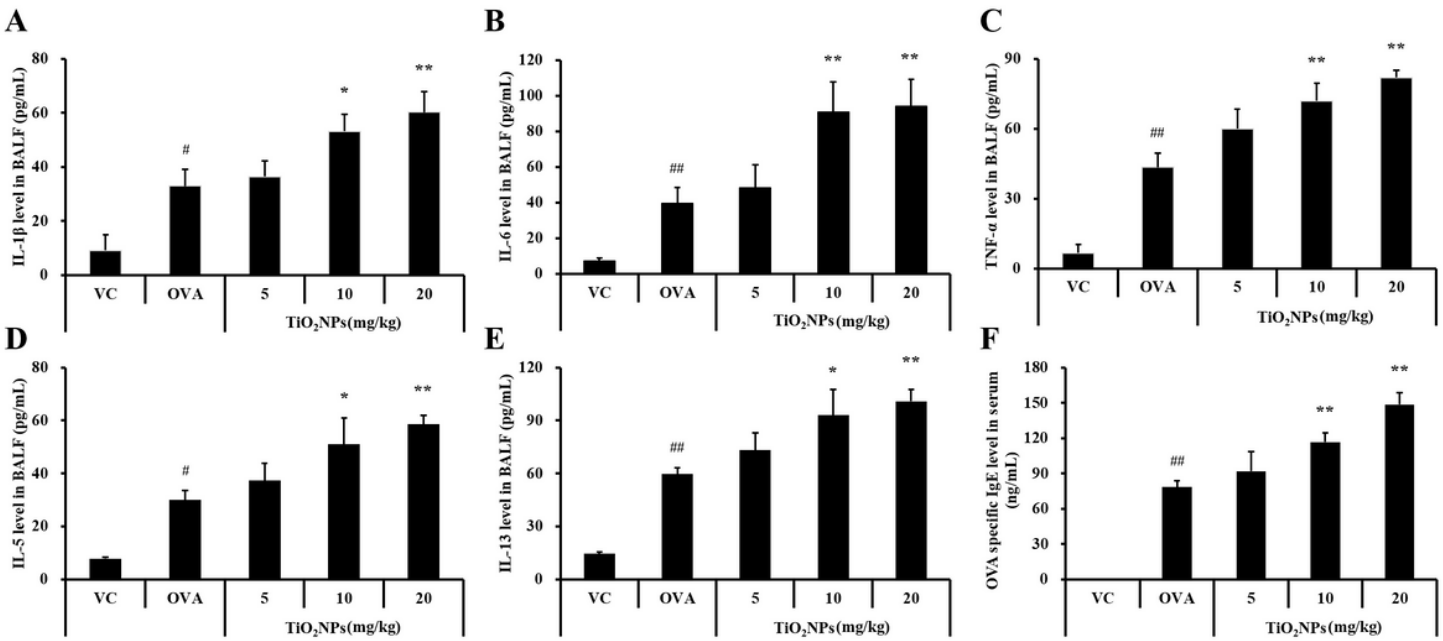

Figure 3

Effects of TiO2NPs exposure on cytokines levels in BALF and OVA-specific IgE levels in serum. a IL-1β level in BALF. b IL-6 level in BALF. c TNF-α level in BALF. d IL-5 level in BALF. e IL-13 level in BALF. f OVA-specific IgE level in serum. VC, PBS intranasal instillation; OVA, OVA challenge + PBS intranasal instillation; TiO2NPs 5, 10, and 20, OVA challenge + 5, 10, and 20 mg/kg of TiO2NPs intranasal instillation, respectively. Data are represented as means ± SD, n = 6. # $p < 0.05$, ## $p < 0.01$, significantly different from the VC group; * $p < 0.05$, ** $p < 0.01$, significantly different from the OVA group.

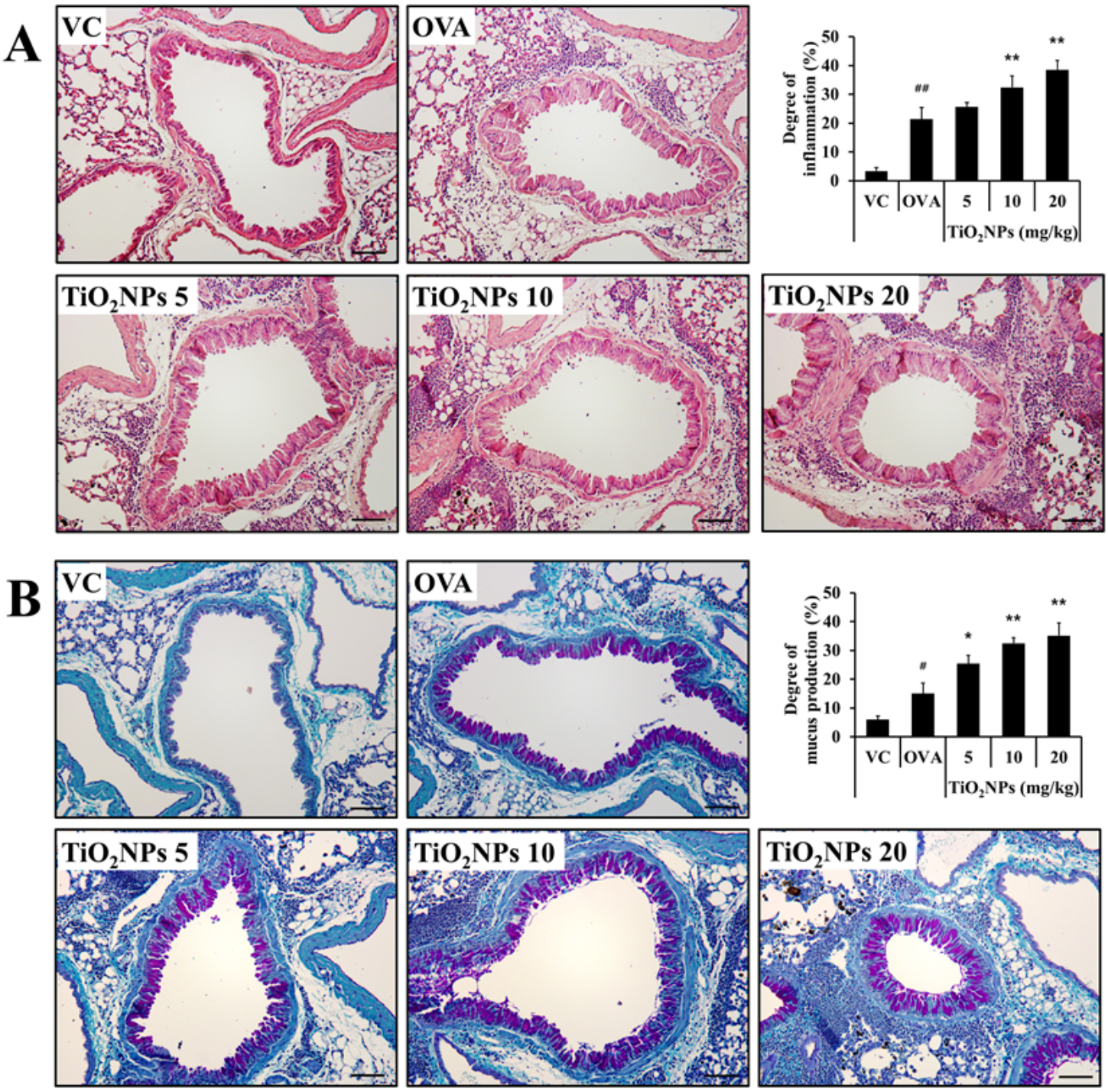

Figure 4

Effects of TiO2NPs exposure on inflammatory cell infiltration and mucus production in the lungs. a Lung tissue stained with hematoxylin and eosin (× 200). b Lung tissue stained with periodic acid-Schiff stain (× 200). VC, PBS intranasal instillation; OVA, OVA challenge + PBS intranasal instillation; TiO2NPs 5, 10, and 20, OVA challenge + 5, 10, and 20 mg/kg of TiO2NPs intranasal instillation, respectively. Data are represented as means ± SD, n = 6. ## $p < 0.01$, significantly different from the VC group; * $p < 0.05$, ** $p < 0.01$, significantly different from the OVA group. Bar = 50 μm.

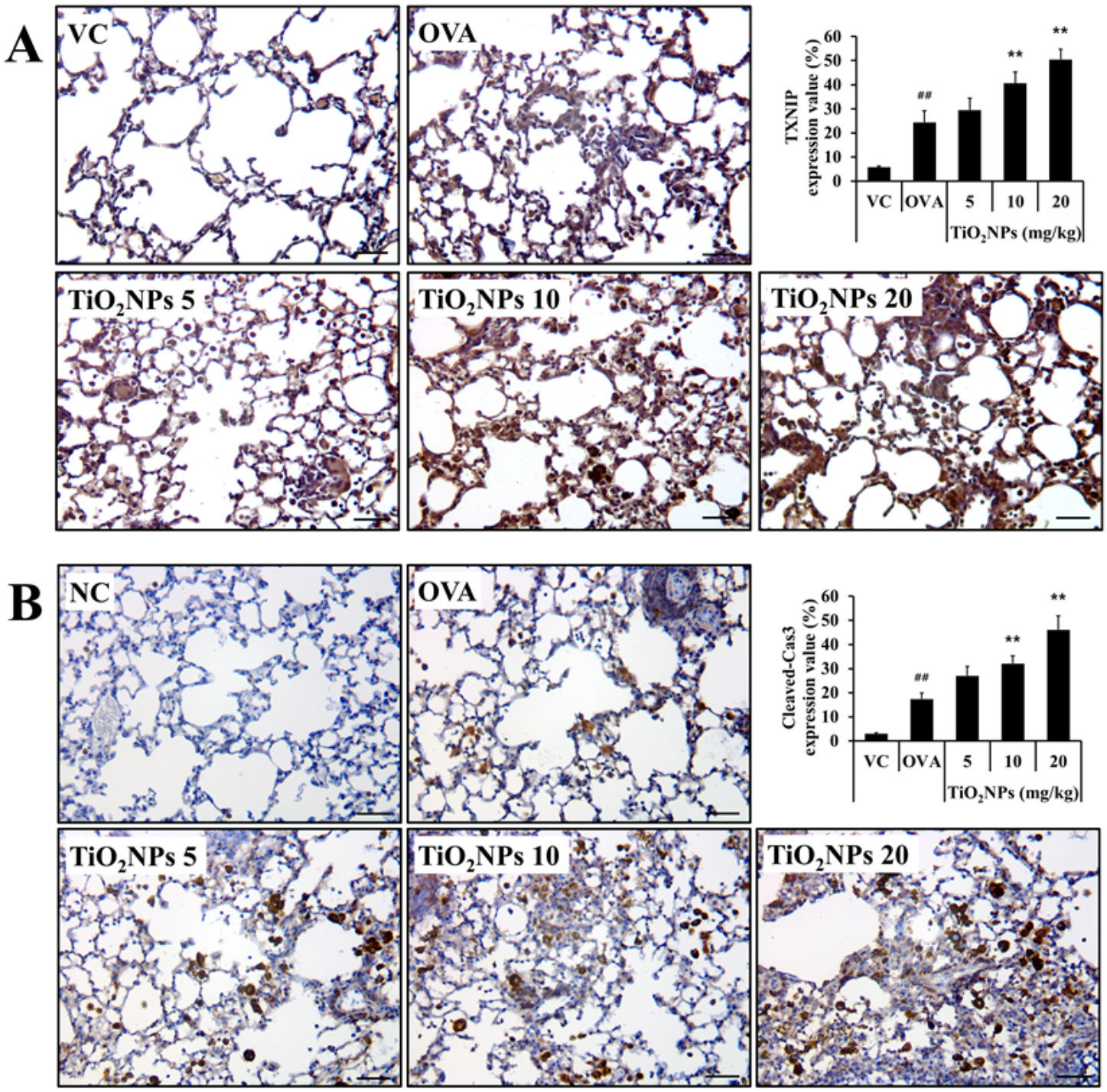

Figure 5

Effects of TiO2NPs exposure on the expression of TXNIP and cleaved-Cas3 in the lungs. a Expression of TXNIP (× 400, alveolar). b Expression of cleaved-Cas3 (× 400, alveolar). VC, PBS intranasal instillation; OVA, OVA challenge + PBS intranasal instillation; TiO2NPs 5, 10, and 20, OVA challenge + 5, 10, and 20 mg/kg of TiO2NPs intranasal instillation, respectively. Data are represented as means ± SD, n = 6. ## $p < 0.01$, significantly different from the VC group; ** $p < 0.01$, significantly different from the OVA group. Bar = 50 μm.

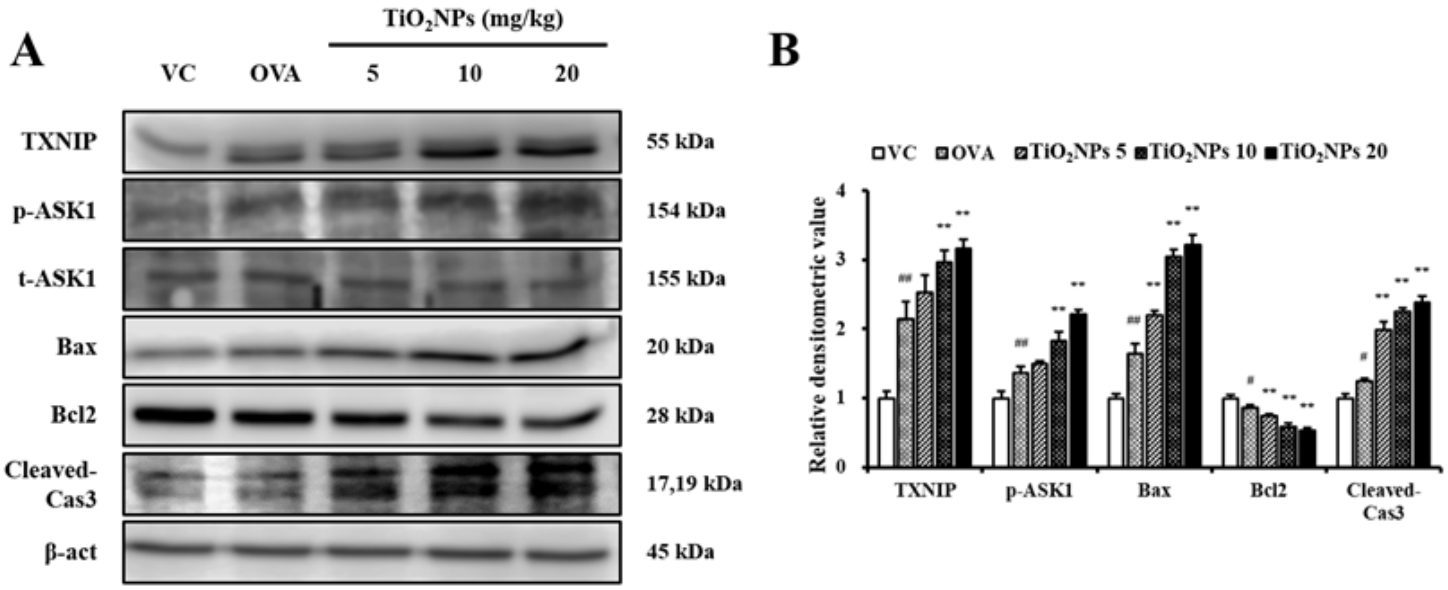

Figure 6

Effects of TiO2NPs exposure on the expression of TXNIP, p-ASK1, t-ASK1, Bax, Bcl2, and cleaved-Cas3 in the lungs. a Protein expression was determined using western blotting. b Relative densitometric values of protein expression. VC, PBS intranasal instillation; OVA, OVA challenge + PBS intranasal instillation; TiO2NPs 5, 10, and 20, OVA challenge + 5, 10, and 20 mg/kg of TiO2NPs intranasal instillation, respectively. Data are represented as means ± SD, n = 6. # $p < 0.05$, ## $p < 0.01$, significantly different from the VC group; ** $p < 0.01$, significantly different from the OVA group.

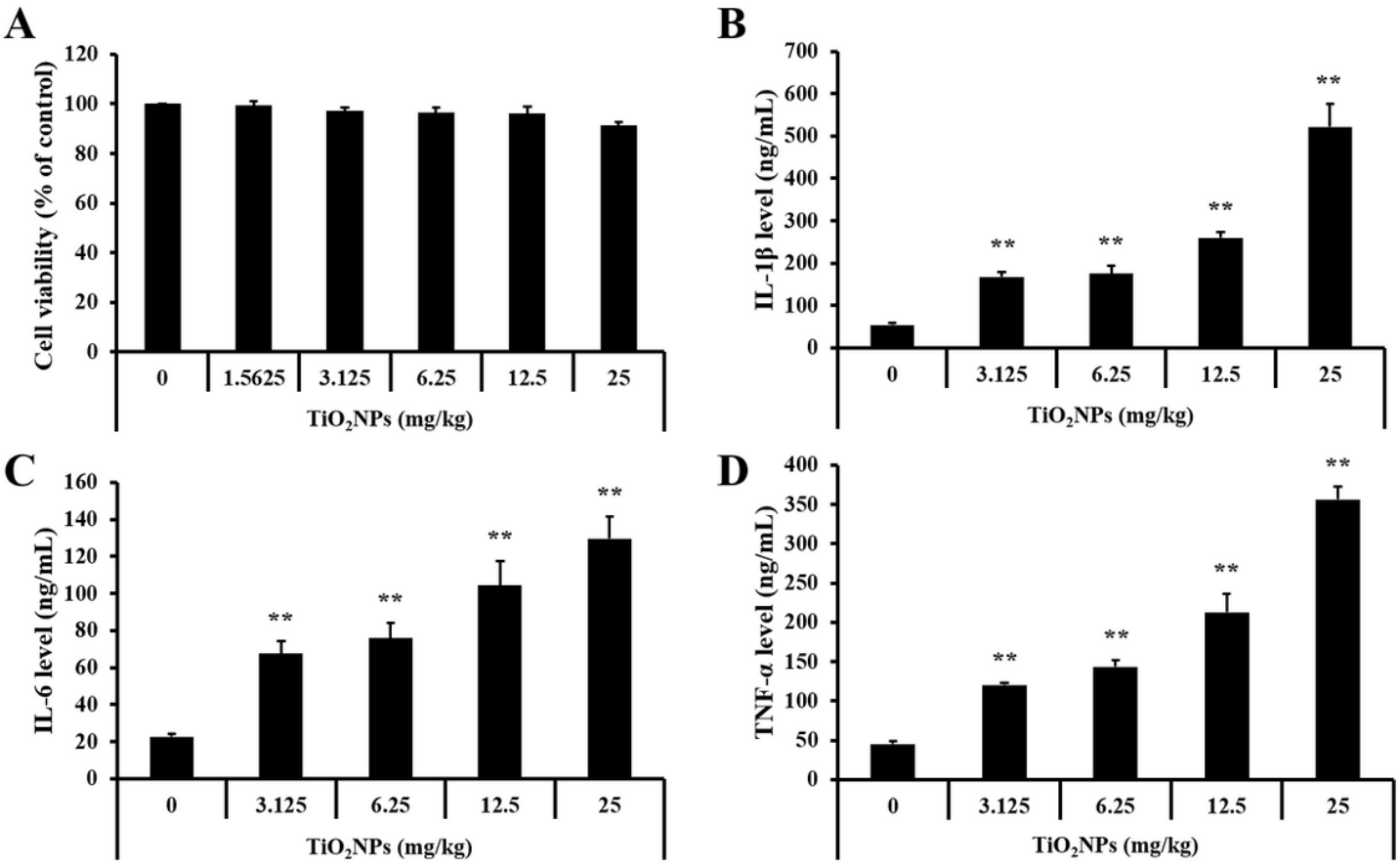

Figure 7

Effects of TiO2NPs treatment on cell viability and inflammatory cytokines in NCI–H292 cells. a Cell viability. b IL-1β level. c IL-6 level. d TNF-α level. Control, PBS treatment; 1.5625, 3.125, 6.25, 12.5, and 25 μg/mL of TiO2NPs treatment; respectively. Data are represented as means ± SD, n = 3. ** $p < 0.01$, significantly different from the control group.

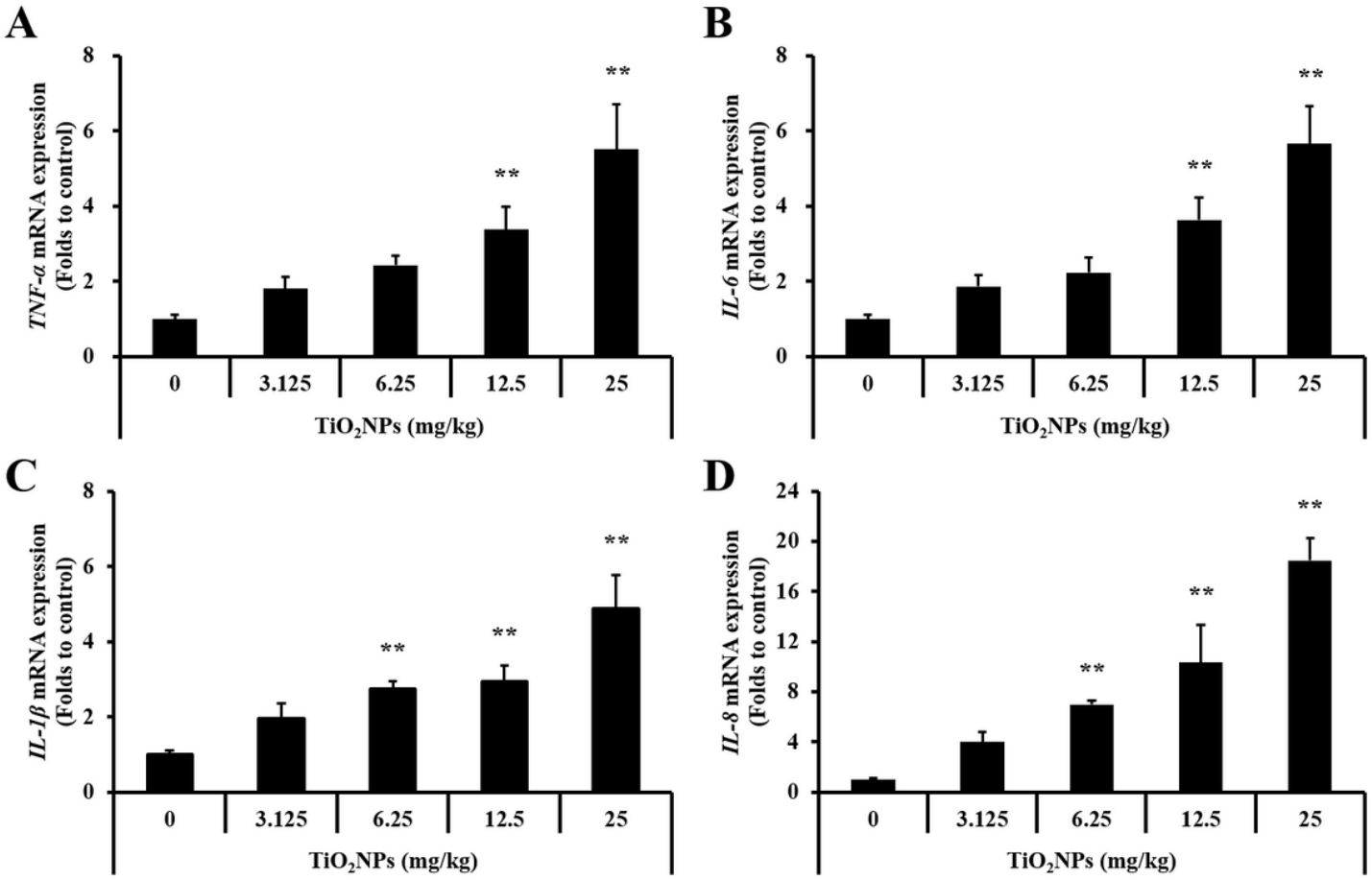

Figure 8

Effects of TiO2NPs treatment on mRNA expression of inflammatory cytokines measured by qRT-PCR in NCI–H292 cells. a TNF-α mRNA expression. b IL-6 mRNA expression. c IL-1β mRNA expression. d IL-8 mRNA expression. Control, PBS treatment; 3.125, 6.25, 12.5, and 25 μg/mL of TiO2NPs treatment; respectively. Data are represented as means ± SD, n = 3. ** $p < 0.01$, significantly different from the control group.

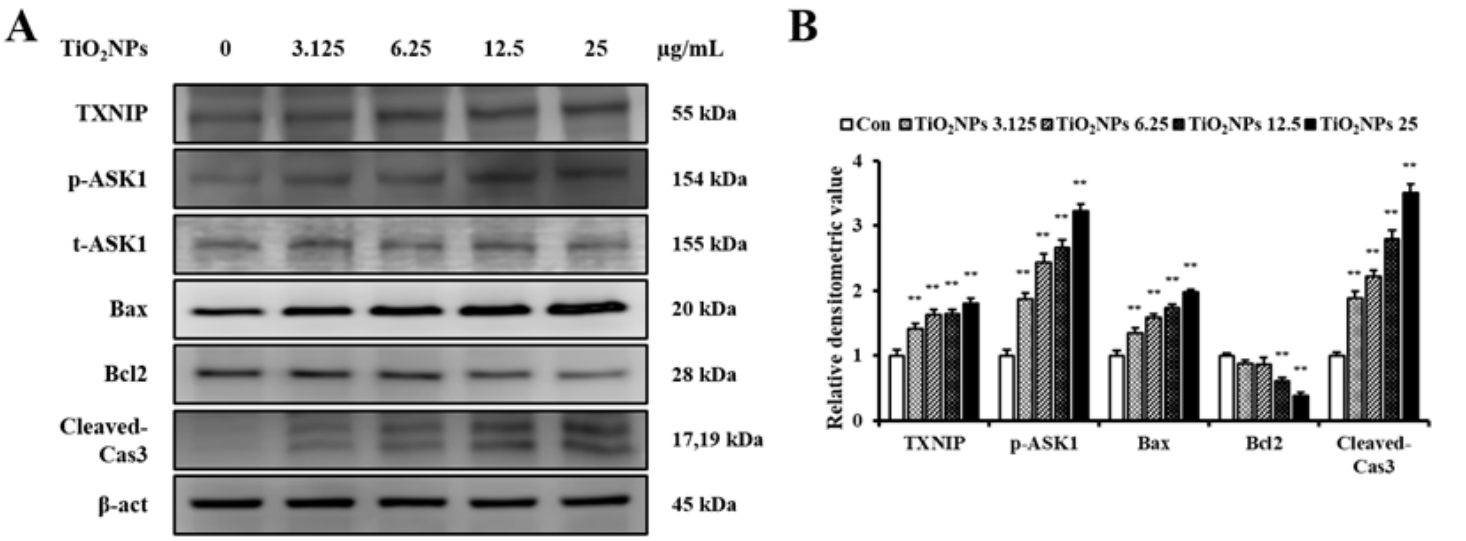

Figure 9

Effects of TiO2NPs treatment on the expression of TXNIP, p-ASK1, t-ASK1, Bax, Bcl2, and cleaved-Cas3 in NCI–H292 cells. a Protein expression was determined using western blotting. b Relative densitometric values of protein expression. Control, PBS treatment; 3.125, 6.25, 12.5, and 25 μg/mL of TiO2NPs treatment; respectively. Data are represented as means ± SD, n = 3. ** $p < 0.01$, significantly different from the control group.

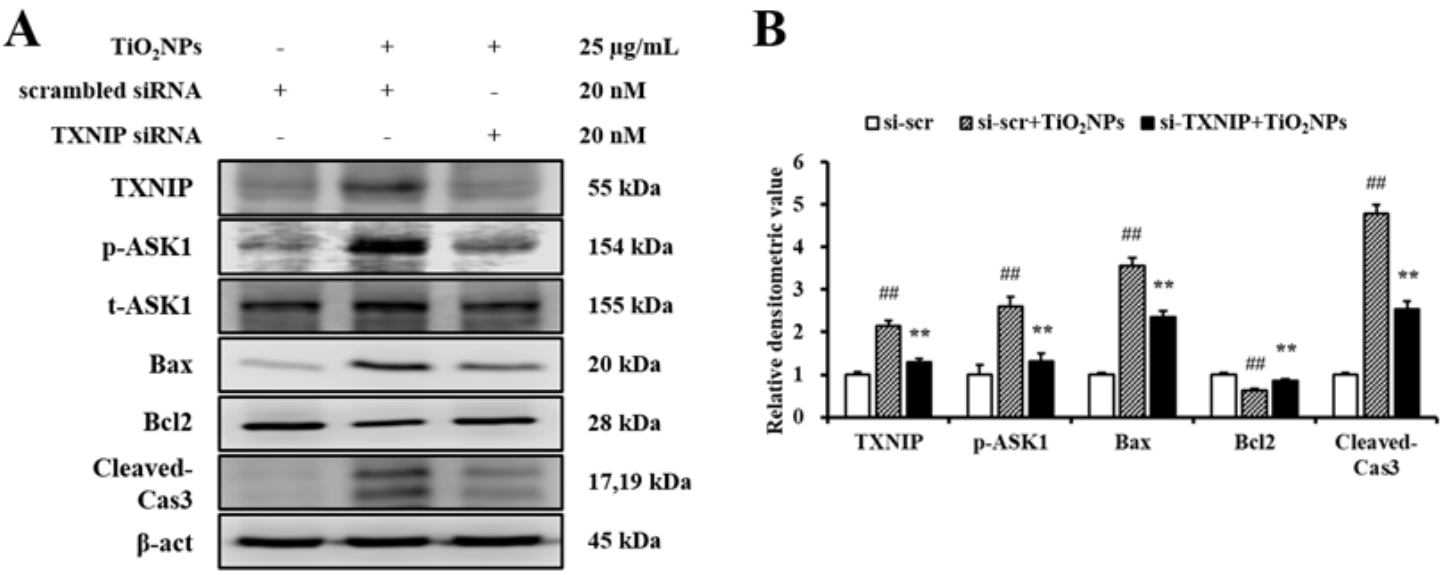

Figure 10

Effects of knockdown of TXNIP on TiO2NPs-induced apoptosis in NCI–H292 cells. a Proteins expression by western blotting. b Relative densitometric values of protein expression. Si-scr, scrambled siRNA 20 nM treatment; si-scr+TiO2NPs, scrambled siRNA 20 nM + TiO2NPs 25 μg/mL treatment; si-TXNIP+TiO2NPs, TXNIP siRNA 20 nM + TiO2NPs 25 μg/mL treatment. Data are represented as means ± SD, n = 3. ## p <

0.01, significantly different from the si-scr group; ** p < 0.01, significantly different from the si-scr+TiO2NPs group.

Supplementary Files

This is a list of supplementary files associated with this preprint. Click to download.

- SupplMaterial.doc